Progress In Electromagnetics Research, Vol. 184, 98–108, 2025

(Received 18 November 2025, Accepted 15 December 2025, Scheduled 25 December 2025)

Air-Processed Perovskite Solar Cells: Progress, Challenges, and Perspectives

(*Invited Paper*)

Zhicheng Guan[1, †], Binghan Li[2, †], Tingwei Ao[1, †], Zhifang Shi[2, *], Guang Yang[1, *], and Gang Li[1, *]

[1] *Department of Electrical and Electronic Engineering, Photonic Research Institute (PRI)*
Research Institute of Smart Energy (RISE), Research Institute for Advanced Manufacturing (RIAM)
The Hong Kong Polytechnic University, Hung Hom, Kowloon, Hong Kong, China
[2] *Faculty of Materials Science and Energy Engineering, Shenzhen University of Advanced Technology, Shenzhen, China*

ABSTRACT: With increasing demand for renewable energy, perovskite solar cells (PSCs) have emerged as a promising alternative due to their high efficiency and solution-based manufacturing processes. However, the fabrication of PSCs in ambient conditions, as opposed to inert environments, remains challenging due to environmental factors such as moisture and oxygen that degrade perovskite materials. Developing air-processed PSCs is therefore critical for reducing fabrication cost, simplifying manufacturing infrastructure, and enabling scalable production compatible with industrial processes. Moreover, air processing represents a key step toward realistic deployment, bridging the gap between laboratory demonstrations and commercial applications. This perspective discusses the progress of air-processed PSCs, highlights the environmental challenges related to stability and performance, and outlines potential strategies for future research, including precursor chemistry, solvent and additive engineering, and interface optimization. In addition, emerging scalable deposition techniques, automated platforms, and machine learning-assisted control are expected to accelerate device optimization and reproducibility. Despite remaining challenges, commercializing air-processed PSCs is increasingly viable, promising a sustainable and efficient approach for solar energy technology.

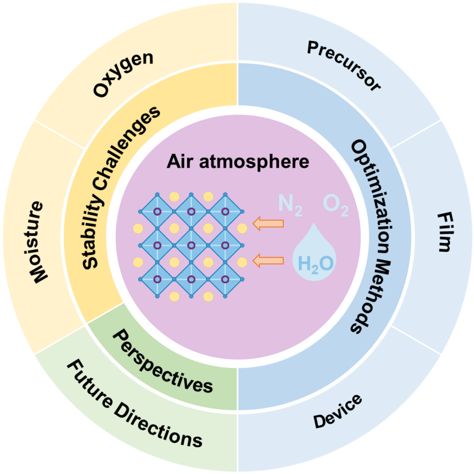

1. INTRODUCTION

Renewable energy sources are gaining significant attention with the growing global challenges of climate change and energy scarcity [1]. Solar power has seen a strong rise in demand, driving increased interest in new and cost-effective technologies for next-generation photovoltaics like perovskite solar cells (PSCs) [2]. PSCs stand out as highly promising candidates for next-generation photovoltaic technologies due to their high power conversion efficiency (PCE), solution-processed manufacturing, and tunable optoelectronic properties [3, 4]. Since their debut in 2009 [5], single-junction PSCs have witnessed a rapid evolution in efficiency, reaching certified values over 27% [6] within just over a decade. While single-junction silicon solar cells have achieved an impressive efficiency of 27.80% [7], approaching the theoretical Shockley-Queisser limit of about 29.40%, further improvements are becoming increasingly difficult as they approach the thermodynamic detailed balance limit [8]. In addition, their energy-intensive production and related carbon emissions highlight the need for new processing methods and device designs. These factors have accelerated the search for alternative photovoltaic technologies like PSCs. However, the most highly efficient PSCs are fabricated under inert atmospheres or controlled humidity to ensure film quality [9], which limits their scalability and increases production cost.

In light of the above, air-processed PSCs have garnered increasing attention as a more practical approach for industrial-scale manufacturing. As a result, recent advances in fabrication methods and modulation strategies have significantly enhanced the development of high-performance air-processed PSCs [10]. Techniques such as slot-die coating, screen printing, spray coating, and inkjet printing have been successfully implemented for large-scale photovoltaic devices [11]. However, PSCs are highly sensitive to the surrounding environment during fabri-

---

* Corresponding authors: Zhifang Shi (zf.shi@suat-sz.edu.cn); Guang Yang (guang.yg.yang@polyu.edu.hk); Gang Li (gang.w.li@polyu.edu.hk).

† These authors contributed equally to this work.

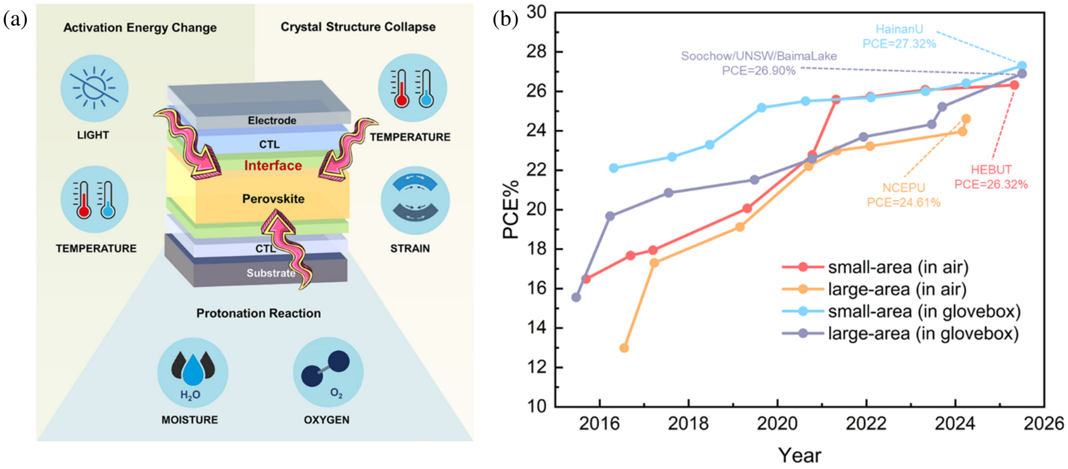

FIGURE 1. (a) Schematic illustration of key environmental factors — including moisture, oxygen, light, temperature — that govern perovskite film formation and stability during ambient fabrication. Reproduced with permission from Ref. [19], Copyright 2023 Elsevier. (b) Chronological evolution of the champion PCE of small-area ($\sim 0.1\,\mathrm{cm}^2$) and large-area ($\sim 1\,\mathrm{cm}^2$) PSCs fabricated in ambient air and glovebox environments. (HainanU (Hainan University), Soochow (Soochow University), UNSW (University of New South Wales), BaimaLake (Baima Lake Laboratory), HEBUT (Hebei University of Technology), NCEPU (North China Electric Power University)).

cation, making ambient production challenging [12]. For perovskite compositions, charge-transport layers and their interfaces can be affected by air. Various strategies have been explored to make air-processed PSCs more efficient, stable, and reproducible, including compositional tuning, additive incorporation, solvent engineering, and surface modification [13–18]. Figure 1 illustrates the environmental factors affecting PSCs and recent performance trends of both small-area and large-area PSCs fabricated under ambient air versus glovebox conditions. Encouragingly, the performance gap between devices fabricated in air and those processed in inert atmospheres is narrowing. Given that material costs constitute only a fraction of the total cost of PSC production, with the majority of expenses stemming from processing and equipment, ambient fabrication offers cost reductions by eliminating the need for gloveboxes, gas purification systems, and a continuous inert gas supply. This enhances the economic feasibility of the large-scale manufacturing of PSCs. From this perspective, we discuss the challenges of perovskite stability in ambient air, recent advancements in air-processing methods, and future research directions.

2. STABILITY CHALLENGES OF PEROVSKITES IN AMBIENT AIR FABRICATION

High-quality perovskite films are essential for ensuring both the stability and efficiency of PSCs. Such films typically exhibit high surface coverage, large grain sizes, low defect concentrations, and uniform crystal orientation [20, 21]. These characteristics collectively underpin their superior performance. However, PSCs exhibit pronounced sensitivity to environmental factors such as moisture, oxygen, light, and temperature, all of which can influence their performance and long-term stability [22]. Oxygen and water have been proven to be the most important external elements leading to the degradation of PSCs [19]. Accordingly, the following section examines the roles of water and oxygen in shaping the quality of perovskite during the fabrication of PSCs under ambient conditions.

$CH_3NH_3PbI_3$ ($MAPbI_3$) is the archetypal perovskite in PSCs, but the hygroscopic methylammonium cation (MA^+) makes it highly moisture-sensitive, accelerating degradation [23]. Water penetrates along grain boundaries to form a reversible monohydrate (Eq. (1)) and, under high humidity, a zero-dimensional dihydrate (Eq. (2)) that can decompose to volatile MAI and residual PbI_2 (Eq. (3)), causing lattice expansion, grain-boundary separation, and impaired charge transport; these pathways and their light-assisted progression have been documented by XRD and optical studies [24–27]. PbI_2 accumulation also raises solubility and toxicity concerns [28, 29].

$$\mathrm{MAPbI_3 + H_2O \leftrightarrow MAPbI_3 \cdot H_2O} \tag{1}$$

$$\begin{aligned}&(4-n)\mathrm{MAPbI_3} + n\mathrm{MAPbI_3 \cdot H2O} + (2-n)\mathrm{H_2O}\\&\leftrightarrow \mathrm{MA_4PbI_6 \cdot 2H_2O + 3PbI_2}\end{aligned} \tag{2}$$

$$\mathrm{MA_4PbI_6 \cdot 2H_2O \leftrightarrow PbI_2 + 4MAI + 2H_2O} \tag{3}$$

Beyond its role in degradation, water exerts stage-specific effects during fabrication, influencing nucleation, intermediate phase evolution, and final film morphology. In one-step spin coating, excessive humidity accelerates nucleation, producing poor coverage and reduced device stability, while controlled relative humidity (RH) yields more uniform films [30, 31]. Moderate humidity during annealing can promote Ostwald ripening, enlarging grains and improving crystallinity, though sometimes at the cost of coverage [32, 33]. In two-step processes, moisture during PbI_2 formation lowers precursor supersaturation, reducing nucleation density and producing larger, rougher PbI_2 grains via adsorption and hydrogen bonding, which can harm morphology [31]; however, residual water can aid MAI-PbI_2 conversion in the subsequent salt step [34, 35]. Thus, the best practice is low humidity for the initial PbI_2

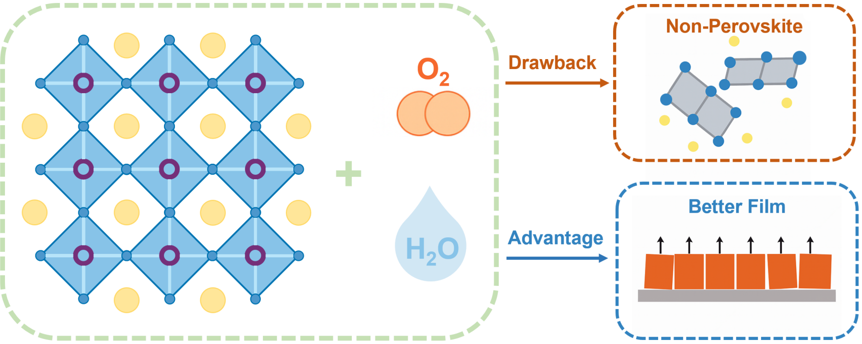

FIGURE 2. Dual role of oxygen and water for the perovskite film: Degradation of perovskites or better film crystallization.

deposition and controlled, moderate humidity during conversion and annealing [36]. At scale, humidity plays a dual role: low RH limits dissolution and grain growth, excessive RH causes over-dissolution and water accumulation at grain boundaries, while intermediate RH optimizes PbI_2 solubility, promotes grain growth, suppresses pinholes, and helps passivate grain boundaries — making humidity a key tunable process parameter [37].

Oxygen also exhibits a dual role during the fabrication of PSC [38]. $MAPbI_3$ degrades in O_2, forming charge barriers via reactions with MA^+ and increasing defect mobility and electron traps [39, 40]. Photoexcited electrons accelerate oxygen-mediated degradation: in the dark, $MAPbI_3$ can oxidize to PbI_2 (Eq. (4)), while under illumination, superoxide (O_2) formed from O_2 reacts with photoexcited $MAPbI_3$* to drive deprotonation and decomposition (Eq. (5)) [41]. Iodine vacancies and grain boundaries promote O_2 formation and diffusion; thus, films with smaller grains (more boundaries) generate more superoxide and degrade faster. Inorganic perovskites ($CsPbX_3$) follow different oxidation pathways depending on O_2 content (Eqs. (6)–(8)) [42]. Photoexcited $CsPbBr_3$ can transfer electrons to metal oxides (TiO_2, SnO_2, ZnO), which then reduce O_2 to O_2^- (Eq. (9)), causing hole accumulation in the perovskite and accelerating oxidation [43]. Chemisorbed oxygen can also induce interstitial oxygen defects in compositions like $CsPbI_2Br$, further compromising stability [44].

$$4CH_3NH_3PbI_3 + O_2 \rightarrow 4PbI_2 + 2I_2 + 2H_2O \\ +4CH_3NH_2 \tag{4}$$

$$4CH_3NH_3PbI_3 * +O_2^- \rightarrow 4PbI_2 + 2I_2 + 2H_2O \\ +4CH_3NH_2 \tag{5}$$

$$CsPbX_3 + \frac{1}{2}O_2 \rightarrow \frac{1}{2}Cs_2O + \frac{1}{2}X_2 + PbX_2 \tag{6}$$

$$CsPbX_3 + \frac{1}{2}O_2 \rightarrow CsX + X_2 + PbO \tag{7}$$

$$CsPbX_3 + \frac{3}{4}O_2 \rightarrow \frac{1}{2}Cs_2O + \frac{3}{2}X_2 + PbO \tag{8}$$

$$CsPbBr_3(h^+) + TiO_2(e^-) + O_2 \rightarrow CsPbBr_3(h^+) \\ +TiO_2 + O_2^- \tag{9}$$

Despite these drawbacks, oxygen can also play a beneficial role in PSC fabrication. Brenes et al. reported that air exposure during one-step deposition can reduce trap density [45]. This effect is attributed to superoxide formation at iodide vacancies, which passivates shallow surface states and suppresses ion migration. In two-step processes, Ren et al. found that oxygen can interact at perovskite-interface regions to passivate defects [46], while Cheng et al. demonstrated carrying out the two-step method in an atmosphere with elevated oxygen levels and high RH = 70% with improved moisture resistance [47]. Thus, an appropriate oxygen concentration can enhance the crystallinity and stability of perovskite. Oxygen also influences device properties during annealing. It was observed that oxygen treatment during this stage reduces trap density, prolongs carrier lifetime, suppresses non-radiative recombination, and improves device performance compared with inert-gas annealing [46].

Taken together, moisture and oxygen exhibit pronounced stage-dependent dual roles (shown in Figure 2) during the ambient fabrication of perovskite solar cells. While excessive or uncontrolled exposure accelerates chemical degradation through hydration- and oxidation-driven pathways, precisely regulated introduction at specific processing stages can promote crystallization, defect passivation, and interfacial stabilization. Consequently, rational control over exposure timing, concentration, and processing sequence is essential to harnessing their beneficial effects while suppressing degradation. This understanding provides a coherent framework for designing robust air-processing strategies.

3. RECENT PROGRESS IN AIR-PROCESSED PSCS

Recent advances in air-processed PSCs can be divided into precursor chemistry, film crystallization control, and device optimization (shown in Figure 3 and Table 1). Perovskite precursors in air are prone to iodide oxidation ($I^- \rightarrow I_2/I_3^-$) and deprotonation of organic cations, leading to halide/Pb vacancies, energetic disorder, and shallow non-radiative traps. These reactions precondition films toward poor crystallinity and low device performance. Countermeasures typically involve redox control and ionic-pair stabilization. Benzylhydrazine hydrochloride reconverts I_2 to I^- [48], while DMAFo stabilizes iodide and organic cations through coordination and hydrogen bonding, improving crystallinity and reducing defects [49]. Tian et al. incorporated bio-derived chitin polymers in the two-step process [50]. Chitin forms coordination and hydrogen bonds with PbI_2 and organic salts, stabilizing inks against

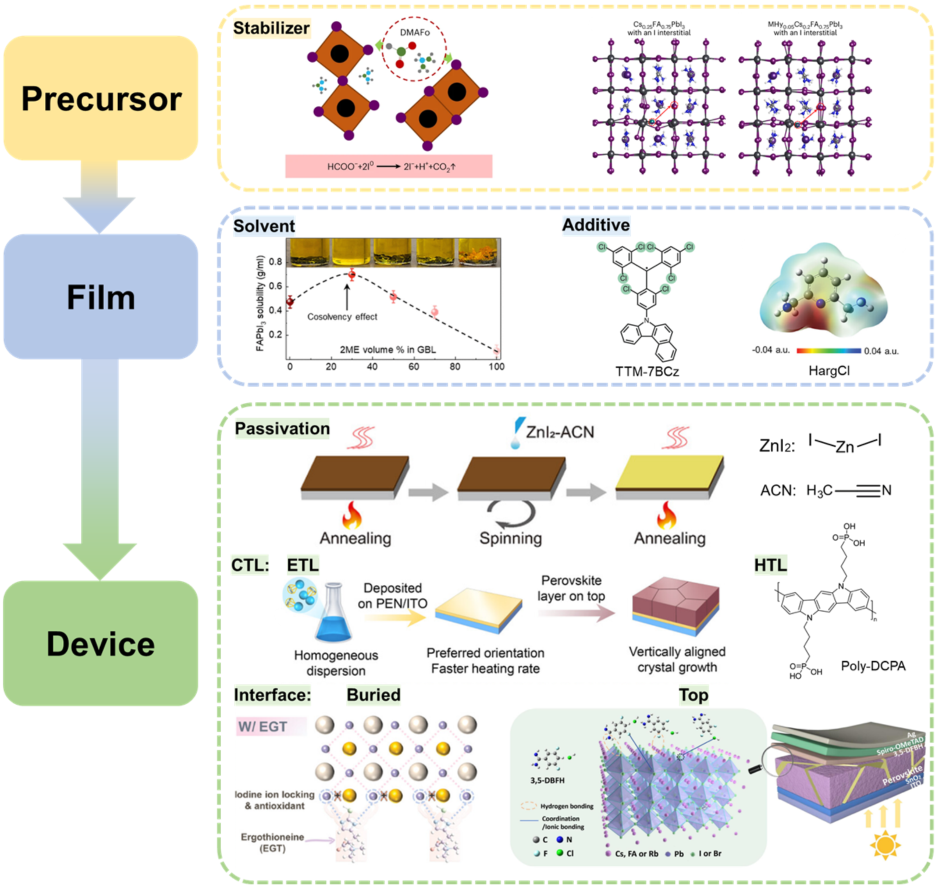

FIGURE 3. Optimization strategies for air-processed PSCs. The figure groups methods by scale: precursor stabilization (yellow), film crystallization (blue), and device optimization (green). Precursor stabilizer: a protective effect of DMAFo in the precursor under air conditions [49] and reductive MHy^+ molecular, which can suppress iodide oxidation and halide segregation [51]. Reproduced with permission from Refs. [49] and [51], Copyright 2024 Springer Nature and 2025 Springer Nature. Film crystallization optimization includes solvent and additive engineering. Solvent engineering: Cosolvency effect for the solubility of $FAPbI_3$ in 2ME/GBL mixtures as a function of 2ME fraction at 90°C [53]. Reproduced with permission from Ref. [53], Copyright 2025 American Chemical Society. Additive engineering: Molecular structure of the TTM-7BCz additive [59] and electrostatic surface potential map of HargCl additive [60]. Reproduced with permission from Refs. [59] and [60], Copyright 2024 The American Association for the Advancement of Science and 2025 Wiley-VCH GmbH. Device optimization encompasses passivation of the perovskite layer, enhancement of the charge transport layer (CTL), and interface engineering for both the buried and top surfaces. Passivation: ZnI_2 in acetonitrile (ACN) post-treatment on perovskite films [62]. Reproduced with permission from [62], Copyright 2025 Wiley-VCH GmbH. CTL improvement contains doping SnO_2 ETL via DAC-AA [66] and novel HTL poly-DCPA [67]. Reproduced with permission from Refs. [66, 67], Copyright 2025 Wiley-VCH GmbH and 2024 Royal Society of Chemistry. Interface engineering: EGT at the SnO_2/perovskite interface [68] and 3,5-DFBH at the perovskite/HTL interface [70]. Reproduced with permission from [68, 70]. Copyright 2024 Wiley-VCH GmbH and 2024 Elsevier.

degradation, accelerating solid-liquid conversion, and yielding oriented, defect-suppressed films. Our group introduced reductive methylhydrazinium (MHy^+), which coordinates with Pb, suppresses iodide oxidation and halide segregation, and raises the migration barrier [51]. This yielded a wide-bandgap (WBG) PSC with 23.30% PCE and a record-low 0.37 V voltage loss; mini-modules achieved 19.80% efficiency in ambient air, retaining 94% after 700 h at 55 ± 5°C.

Film crystallization dynamics also play critical roles in air-processed PSCs. Process parameters strongly influence perovskite crystallization under ambient conditions. Using an automated deposition platform (SPINBOT), Zhang et al. identified organic halide dripping speed as a critical variable, about 50 μL/s, that minimized PbI_2 residues and yielded dense, large-grained films [52]. Devices fabricated using this protocol exceeded 23.00% PCE and retained more than 93% efficiency after 1200 hours of photo-thermal stress, highlighting the automation for reproducible, additive-free fabrication. Solvent engineering further optimizes the crystallization process. A cosolvency effect for $FAPbI_3$ in γ-butyrolactone (GBL)/2-methoxyethanol (2ME) mixtures enhanced solubility. Mixing GBL with 2ME disrupts the hydrogen bonding of 2ME, allowing its hydroxyl/ether groups to solvate the precursor more effectively. The resulting shift in solubility lowers instantaneous supersaturation during high-temperature crystallization, suppresses δ-phase formation, and reduces nucleation density, enabling space-confined growth of undoped α-$FAPbI_3$ thin single crystals in air [53]. Another strategy replaced isopropanol with less volatile isobutanol, slowed evaporation, suppressed the δ-phase, and broadened

TABLE 1. Representative air-processed PSCs demonstrations. Optimization level, device architecture, coating method, fabrication condition (typical RH), reported PCE, and reference are listed.

Optimization level	Device architecture	Coating method	Fabrication condition	PCE (%)	Ref.
Precursor	p-i-n; DMAFo-stabilized precursor	Spin coating	Ambient air 35–50 RH%	24.72%	Nature Energy 2024 [49]
Precursor	p-i-n; Reductive MHy^+ cation for WBG PSCs	Blade coating	Ambient air	23.30%	Nature Sustainability 2025 [51]
Film	p-i-n; GBL/2-ME cosolvency	Spin coating	Ambient air	21.56%	JACS 2025 [53]
Film	n-i-p; Additives improve crystallization	Spin coating	Ambient air 20–60 RH%	24.50%	Science 2024 [59]
Film	p-i-n; Additives improve the film	Spin coating	Ambient air	25.05%	Adv. Energy Mater. 2025 [60]
Device	p-i-n; Passivation (ZnI_2 post-treatment)	Spin coating	Ambient air 60 ± 10 RH%	25.20%	Angew. Chem. Int. Ed. 2025 [62]
Device	p-i-n; Dual-site passivation (APCl)	Spin coating	Ambient air	26.32%	Energy Environ. Sci. 2025 [63]
Device	n-i-p; SnO_2 doping with DAC-AA	Spin coating	Ambient air	23.87%	Adv. Mater. 2025 [66]
Device	p-i-n; Poly-DCPA hole transporter	Blade coating	Ambient air	24.90%	Energy Environ. Sci. 2025 [67]
Device	n-i-p; Buried-interface engineering (EGT)	Spin coating	Ambient air	25.13%	Adv. Mater. 2024 [68]
Device	n-i-p; Top-interface engineering (3,5-DFBH)	Spin coating	Ambient air	24.57%	Chem. Eng. J. 2024 [70]
Device	n-i-p; Monolithic perovskite-organic hybrid tandem solar cells	Spin coating	Ambient air	23.07%	Energy Environ. Sci. 2024 [72]
Device	p-i-n; Perovskite-organic tandem solar cells	Blade coating	Ambient air	24.40%	Adv. Energy Mater. 2025 [73]

the RH window from 20% to 80%, enabling devices up to 25.10% PCE with $> 1000\,\mathrm{h}$ stability [54]. Water and alcohol based solvents are gaining attention as green alternatives for ambient-air perovskite processing [55, 56]. Compared to traditional toxic solvents, water and short-chain alcohols reduce health and environmental risks while offering new ways to control crystallization. A previous study reported that water-based systems, such as $Pb(NO_3)_2/H_2O$, can produce high-quality films when combined with additives or light modulation, achieving PCEs of 23.74% under ambient conditions [57]. These strategies help regulate nucleation, improve film coverage, and expand the workable humidity range. Using green solvents also supports scalable coating methods, such as blade and slot-die printing, making them promising for industrial production. Additives can tune crystallization and enhance phase stability. 2-thiazole formamidine hydrochloride molecules slowed crystallization and improved morphology [58]. Hydrophobic radical TTM-7BCz stabilized PbI_2-DMSO complexes, enabling oriented $FAPbI_3$ films at 20–60% RH with 24.50% PCE [59]. A similar approach was reported by Wu et al. [60], who introduced L-homoarginine hydrochloride (HargCl) into the PbI_2 precursor to suppress the formation of hygroscopic $PbI_2\cdot$ xDMSO complexes. HargCl not only displaced residual DMSO through stronger coordination with PbI_2 but also passivated vacancy defects and imparted hydrophobic protection to the perovskite film. This multifunctionality enabled the fabrication of fully air-processed inverted PSCs with a champion PCE of 25.05% and outstanding stability, retaining 96% of their initial efficiency after 500 hours of storage in 20–40% RH.

Beyond crystallization to the device level, films processed in air often retain excess defects and surface instabilities. Strategies target specific vacancies or coordination sites. In inorganic perovskites, Liu et al. exploited ambient moisture to hydrolyze sulfonic acid precursors, which passivated Pb^{2+} defects and improved hydrophobicity. $CsPbI_3$ modules reached 18.22% (certified) with strong environmental stability [61]. Surface cation exchange was demonstrated by Xu et al., who treated films with ZnI_2, partially replacing Pb^{2+} to form a compact PbI_2 shell [62]. This passivated defects, optimized band alignment, and enabled an efficiency of 25.20% under humid air. Dual-site binding was achieved by Lu et al., who introduced heterocycle-functionalized amidinium (APCl) to target both FA^+ and I^- vacancies, reducing recombination and stabilizing interfaces. This strategy yielded 26.83% (certified 26.32%) with excellent durability [63]. Scalable approaches have also been reported. Incorporation of fluorinated quaternary ammonium iodide (FSAI) into precursors stabilized the α-$FAPbI_3$ phase and passivated defects, producing uniform blade-coated films with 24.37% efficiency and 22.00% for modules [64]. Sodium benzene phosphinate (SBP) suppressed iodide oxidation and ion migration during blade-coating at $\sim$60% RH, enabling 22.10% efficiency and $>$ 2000 h air stability [65]. These examples show how molecular passivation also extends to scalable coating methods under humid air.

Interface engineering is also critical for high-performance ambient-processed devices. Optimizations can be implemented in charge transport layers. Ning et al. engineered SnO_2 electron transport layers (ETLs) via doping with DAC-AA molecules, which coordinate with SnO_2 to reduce surface defects and promote preferential (101) and (200) facet orientations better matched to the perovskite (100) plane [66]. This facet control improves charge transfer and suppresses micro-strain, leading to flexible PSCs with efficiencies of 23.87% and remarkable mechanical durability. For hole transport layers (HTLs), Zhao et al. developed the polymer poly-DCPA to improve adhesion between the HTL and the transparent conductive oxide (TCO) in scalable devices [67]. The biphosphonic acid groups in poly-DCPA formed robust anchoring interactions with the TCO surface, simultaneously interacting with the perovskite layer to significantly enhance interfacial stability and film quality. Compared to conventional SAM hole transport layers, poly-DCPA exhibited over four times stronger adhesion, improved conductivity due to its extended conjugated backbone, and broadened the processing window for ambient blade coating. Buried interface engineering has also been extensively explored. Yang et al. introduced ergothioneine (EGT) at the SnO_2/perovskite interface, where EGT chelates uncoordinated Sn^{4+}/Pb^{2+}, anchors iodide ions to suppress their oxidation, reduces interfacial recombination and ion migration, lowers oxygen vacancies in SnO_2, and promotes oriented crystallization with stress relief. This multifunctional approach enabled devices with a record 25.13% efficiency and excellent long-term thermal stability [68]. Zhu et al. proposed an interfacial engineering strategy by introducing tetramethylammonium chloride (TMACL) as a “molecular glue” to strengthen the SnO_2/perovskite interface [69]. TMACL not only stabilized SnO_2 colloidal solutions for uniform blade-coating but also effectively reduced interfacial trap densities and guided ordered perovskite crystal growth. This approach enabled fully air-processed blade-coated PSCs to achieve a champion PCE of 26.11% for small cells and 22.76% for a 57.2 cm^2 module, alongside excellent operational stability exceeding 1500 hours under ISOS-O testing. At the top interface, fluorination-based engineering has also shown great promise. A fluorination-based interface engineering method introduces fluoro-substituted benzamidine hydrochlorides, notably 3,5-difluoro-benzamidine hydrochloride (3,5-DFBH), to effectively passivate cation and halide vacancies via ionic, hydrogen-bonding, and coordination interactions [70]. This treatment also relieves tensile stress at the perovskite/HTL interface, optimizes energy level alignment, and enhances surface hydrophobicity, thereby suppressing both radiative and trap-assisted non-radiative recombination. As a result, devices reach a 24.57% efficiency with outstanding stability under humidity and thermal stress [70]. A dynamic surface reconstruction method was introduced by immersing $CsPbI_2Br$ films in low-polarity organic esters at elevated temperature [71]. The weak solubility of these esters enabled partial dissolution of the superficial lattice, followed by in situ recrystallization into a Br-rich capping layer. This process effectively removed defect-rich nano-impurities, released tensile strain, and strengthened the fragile surface. Devices fabricated using this method achieved 15.37% efficiency in fully air-processed carbon-based n-i-p cells, while maintaining excellent tolerance to moisture and oxygen [71].

Recent progress has demonstrated that the fully ambient fabrication of high-efficiency tandem devices is achievable. Metal-ion-doped all-inorganic WBG front cells processed via dynamic hot-air and paired with passivated ZnO and a ternary organic solar cell rear yielded a small-area 2-terminal tandem of 23.07% (21.82% at 1 cm^2) with minimal Voc loss and sustained stability [72]. Blade-coated ultrawide-bandgap perovskites processed in air were stabilized by a $Pb(SCN)_2$ pseudohalide modulator that increases heterogeneous nucleation, extends the crystallization window, and forms a bottom-enriched passivating gradient; integrating this UWBG front with a ternary organic solar cell rear produced an air-processed tandem at

24.40% (certified 23.10%) and long lifetimes for the UWBG subcell [73].

4. DISCUSSION AND PERSPECTIVES

The progress of air-processed PSCs highlights both remarkable achievements and persistent challenges. On the one hand, a series of material innovations has significantly narrowed the performance gap between air-fabricated and glovebox-processed devices. Recent demonstrations of PCEs exceeding 26% [63] for devices fabricated under ambient conditions underscore the feasibility of scalable, low-cost processing. On the other hand, the intrinsic sensitivity of perovskites to moisture, oxygen, and thermal stress continues to pose serious barriers to long-term device stability and large-scale reproducibility. Among these challenges, ambient moisture proves to be particularly critical. Controlled humidity can aid crystallization, reduce interfacial defects, and stabilize certain perovskite phases, but uncontrolled exposure accelerates degradation. Moisture interacts with organic cations to form hydrated intermediates that disrupt structure and charge transport [74]. Oxygen exacerbates degradation through redox reactions, especially with moisture present, while light accelerates ion migration and generates reactive superoxide [75, 76]. Temperature fluctuations further accelerate these pathways [77]. These sensitivities highlight the need for precise environmental control and robust defect passivation strategies to ensure device durability [19].

Device architecture also plays a central role. Compared to n-i-p devices, studies on air-processed inverted PSCs remain limited and often focus on precursor tuning [48, 49]. Despite advances in thin-film deposition, interfacial issues contribute to the persistent performance gap. For example, moisture and oxygen can adsorb on perovskite surfaces during the interval before ETL evaporation, disturbing subsequent deposition and energy-level alignment [78]. While hydrophobic, electron-conducting capping layers may help, suitable materials remain scarce. Similarly, although SAMs have emerged as promising HTL for p-i-n devices, their amphiphilic nature often leads to aggregation and incomplete coverage on rough ITO substrates under ambient conditions, generating buried-interface defects and instability [79]. Future work should therefore emphasize rational architecture selection and tailored engineering for specific device types and processing environments.

Among perovskite systems, $FAPbI_3$-based and mixed-cation compositions (e.g., FA/Cs/MA) show the best balance between efficiency and tolerance to ambient moisture and oxygen [80]. Their relatively stable α-phase and compatibility with additive, solvent, and surface treatments make them well-suited for air processing [81]. In contrast, inorganic $CsPbX_3$ perovskites offer superior thermal and moisture stability but are more prone to oxidation and require stricter crystallization control and post-treatment to achieve high-quality films in air [82]. Wide-bandgap perovskites represent another critical frontier for tandem applications. Although optimized solvent systems have stabilized WBG films under air, mixed-halide compositions still suffer from segregation and phase collapse [83]. Promising directions include pseudo-halide incorporation, A-site mixing strategies, and interface designs that resist oxidation and hydration [84, 85]. These strategies, proven effective in narrow-bandgap perovskites, must be adapted for WBG systems to ensure stability under ambient processing.

Scaling from small-area cells to modules introduces additional challenges [86, 87]. Quantitatively, champion small-area cells reach 27% PCE while modules typically report lower efficiencies (commonly 20–24%). Key contributors to this gap include local humidity gradients during large-area coating, increased probability of pinholes and shunts across larger areas, and mechanical or thermal stresses introduced during scribing and module integration. Hybrid methods such as sequential PbI_2 evaporation followed by salt-solution conversion offer improved uniformity under ambient conditions [83]. Other methods include meter-scale process control, robust interconnect strategies, and module-level passivation. However, the scalability of these approaches must be validated in terms of cost, throughput, and device reliability [12, 83].

Looking ahead, several directions are particularly promising for advancing the field. On the materials side, the design of perovskite compositions and charge transport layers with intrinsic tolerance to oxygen and moisture, alongside environmentally benign or lead-free alternatives, will be critical for sustainable commercialization. At the device level, multifunctional interface engineering and defect passivation are expected to remain central strategies for suppressing recombination and extending operational durability. Stability under industrially relevant processing conditions, including high-throughput, high-speed deposition and post-deposition thermal or mechanical stress, must be systematically evaluated to ensure consistent device performance beyond the laboratory scale. Process optimization will also benefit from the deployment of automated and high-throughput fabrication platforms, which can systematically identify optimal processing windows and enhance reproducibility across different scales. Parallel efforts in scalable deposition techniques such as blade coating, slot-die coating, and roll-to-roll printing will be essential to bridge the gap between laboratory devices and industrial modules, particularly for flexible and tandem architectures. Furthermore, environmental considerations such as using green solvents, precursor recycling, and effective strategies to mitigate lead leakage must be integrated into future device design.

Ambient processing reduces reliance on controlled-atmosphere gloveboxes but raises occupational and environmental safety concerns that must be addressed for large-scale production. Solvent vapor can pose inhalation and flammability hazards; even low-toxicity solvents require engineering controls such as local exhaust ventilation, vapor recovery systems, and enclosed coating modules to limit exposure. Wet processing and waste streams may release lead-bearing particulates or soluble Pb species. Mitigation strategies include inline wet-waste treatment with Pb sequestration, lead-immobilizing additives or sacrificial binder layers, and immediate encapsulation after deposition to prevent airborne dispersion. Process design should integrate solvent selection (favoring low-vapor-pressure, low-toxicity candidates), engineering controls, and materials strategies to manage both occupational safety and environmental Pb risks. These measures are essential for the safe and scalable deployment of ambient perovskite technologies.

Finally, data-driven approaches hold strong potential. Machine learning can accelerate material discovery, predict defect pathways, and guide interface design. Coupled with in situ monitoring and automated experimentation, AI-assisted control could dynamically regulate humidity, temperature, and crystallization kinetics, ensuring reproducible film quality even in air. Reducing reliance on trial-and-error methods may rapidly optimize scalable deposition protocols. While significant hurdles remain, the trajectory of air-processed PSCs clearly points toward a future where high-performance, stable, and eco-friendly perovskite photovoltaics can be manufactured on a large scale. Bridging the gap between laboratory innovation and industrial application will require collaborative efforts across materials science, chemistry, engineering, and data science. Still, the prospects for commercialization and energy impact are highly promising.

ACKNOWLEDGEMENT

G.Y. acknowledges funding support from the start-up fund provided by PolyU (1-BEBB), PRI strategic Grant (1-CDJ7), RISE strategic Grant (U-CDCC), RIAM critical-mass strategic fund (1-CDLF), and Shenzhen Science and Technology Innovation Commission (No. JCYJ20250604184249064). G.L. acknowledges the financial support from the Research Grants Council of Hong Kong (GRF Grant Nos. 15221320, 15307922, C7018-20G, C4005-22Y), the Hong Kong Innovation and Technology Commission (MHP/020/23), the Hong Kong Polytechnic University (the Sir Sze-yuen Chung Endowed Professorship Fund (8-8480), PRI strategic Grant (1-CD7X), RISE strategic Grant (Q-CDBK).

REFERENCES

[1] Wang, W., M. O. Tade, and Z. Shao, "Research progress of perovskite materials in photocatalysis- and photovoltaics-related energy conversion and environmental treatment," *Chemical Society Reviews*, Vol. 44, No. 15, 5371–5408, 2015.

[2] Tao, J., C. Zhao, Z. Wang, Y. Chen, L. Zang, G. Yang, Y. Bai, and J. Chu, "Suppressing non-radiative recombination for efficient and stable perovskite solar cells," *Energy & Environmental Science*, Vol. 18, No. 2, 509–544, 2025.

[3] Wang, Z., X. Duan, J. Zhang, W. Yuan, D. Qu, Y. Chen, L. He, H. Wang, G. Yang, W. Zhang, Y. Bai, and H.-M. Cheng, "Manipulating the crystallization kinetics of halide perovskites for large-area solar modules," *Communications Materials*, Vol. 5, No. 1, 131, 2024.

[4] Yang, S., W. Fu, Z. Zhang, H. Chen, and C.-Z. Li, "Recent advances in perovskite solar cells: Efficiency, stability and lead-free perovskite," *Journal of Materials Chemistry A*, Vol. 5, No. 23, 11 462–11 482, 2017.

[5] Kojima, A., K. Teshima, Y. Shirai, and T. Miyasaka, "Organometal halide perovskites as visible-light sensitizers for photovoltaic cells," *Journal of the American Chemical Society*, Vol. 131, No. 17, 6050–6051, 2009.

[6] Li, Y., Z. Zheng, X. Zheng, X. Liu, Y. Yang, Y. Zhu, Z. Wang, X. Ren, M. Fu, R. Guo, *et al.*, "Mutual stabilization of hybrid and inorganic perovskites for photovoltaics," *eScience*, 100449, 2025.

[7] Green, M. A., E. D. Dunlop, M. Yoshita, N. Kopidakis, K. Bothe, G. Siefer, X. Hao, and J. Y. Jiang, "Solar cell efficiency tables (Version 66)," *Progress in Photovoltaics*, Vol. 33, No. 7, 795–810, 2025.

[8] Shi, Y., J. J. Berry, and F. Zhang, "Perovskite/silicon tandem solar cells: Insights and outlooks," *ACS Energy Letters*, Vol. 9, No. 3, 1305–1330, 2024.

[9] Cheng, Y., F. So, and S.-W. Tsang, "Progress in air-processed perovskite solar cells: From crystallization to photovoltaic performance," *Materials Horizons*, Vol. 6, No. 8, 1611–1624, 2019.

[10] Wang, J., L. Yuan, H. Luo, C. Duan, B. Zhou, Q. Wen, and K. Yan, "Ambient air processed highly oriented perovskite solar cells with efficiency exceeding 23% via amorphous intermediate," *Chemical Engineering Journal*, Vol. 446, 136968, 2022.

[11] Rong, Y., Y. Ming, W. Ji, D. Li, A. Mei, Y. Hu, and H. Han, "Toward industrial-scale production of perovskite solar cells: Screen printing, slot-die coating, and emerging techniques," *The Journal of Physical Chemistry Letters*, Vol. 9, No. 10, 2707–2713, 2018.

[12] Zou, Y., W. Yu, B. Qu, Z. Chen, M. Wei, and L. Xiao, "Ambient fabrication of perovskites for photovoltaics," *Nature Reviews Materials*, Vol. 10, 400–402, 2025.

[13] Zhang, F. and K. Zhu, "Additive engineering for efficient and stable perovskite solar cells," *Advanced Energy Materials*, Vol. 10, No. 13, 1902579, 2020.

[14] Shi, X., T. Liu, Y. Dou, X. Hu, Y. Liu, F. Wang, L. Wang, Z. Ren, and S. Chen, "Air-processed perovskite solar cells with $> 25\%$ efficiency and high stability enabled by crystallization modulation and holistic passivation," *Advanced Materials*, Vol. 36, No. 31, 2402785, 2024.

[15] Wang, M., H. Sun, L. Meng, M. Wang, and L. Li, "A universal strategy of intermolecular exchange to stabilize α-$FAPbI_3$ and manage crystal orientation for high-performance humid-air-processed perovskite solar cells," *Advanced Materials*, Vol. 34, No. 23, 2200041, 2022.

[16] Ning, L., L. Song, Z. Yao, W.-H. Chen, P. Du, P.-C. Jiang, and J. Xiong, "Intercepting the chelation of perovskites with ambient moisture through active addition reaction for full-air-processed perovskite solar cells," *Advanced Energy Materials*, Vol. 14, No. 36, 2401320, 2024.

[17] Satale, V. V., S. Chowdhury, A. Mohamed, D.-H. Kim, S. Cho, J.-S. Lee, and J.-W. Kang, "Green solvent enabled perovskite ink for ambient-air-processed efficient inkjet-printed perovskite solar cells," *Advanced Functional Materials*, Vol. 35, No. 40, 2503717, 2025.

[18] Mali, S. S., J. V. Patil, J. A. Steele, Y. H. Jung, M. K. Nazeeruddin, and C. K. Hong, "Controlled crystallization and surface engineering of mixed-halide γ-$CsPbI_2Br$ inorganic perovskites via guanidinium iodide additive in air-processed perovskite solar cells," *Materials Today*, Vol. 67, 33–45, 2023.

[19] Li, B., S. Li, J. Gong, X. Wu, Z. Li, D. Gao, D. Zhao, C. Zhang, Y. Wang, and Z. Zhu, "Fundamental understanding of stability for halide perovskite photovoltaics: The importance of interfaces," *Chem*, Vol. 10, No. 1, 35–47, 2024.

[20] Wang, S., T. Yang, Y. Yang, Y. Du, W. Huang, L. Cheng, H. Li, P. Wang, Y. Wang, Y. Zhang, *et al.*, "In situ self-elimination of defects via controlled perovskite crystallization dynamics for high-performance solar cells," *Advanced Materials*, Vol. 35, No. 42, 2305314, 2023.

[21] Shi, P., Y. Ding, B. Ding, Q. Xing, T. Kodalle, C. M. Sutter-Fella, I. Yavuz, C. Yao, W. Fan, J. Xu, *et al.*, "Oriented nucleation in formamidinium perovskite for photovoltaics," *Nature*, Vol. 620,

No. 7973, 323–327, 2023.

[22] Feng, Z., M. He, Z. Li, and X. Hao, "A perspective on spatiotemporal engineering of multidimensional heterointerfaces in perovskite solar cells," *ACS Nano*, Vol. 19, No. 31, 28 003–28 020, 2025.

[23] Gong, X., M. Li, X.-B. Shi, H. Ma, Z.-K. Wang, and L.-S. Liao, "Controllable perovskite crystallization by water additive for high-performance solar cells," *Advanced Functional Materials*, Vol. 25, No. 42, 6671–6678, 2015.

[24] Zuo, S., W. Niu, S. Chu, P. An, H. Huang, L. Zheng, L. Zhao, and J. Zhang, "Water-regulated lead halide perovskites precursor solution: Perovskite structure making and breaking," *The Journal of Physical Chemistry Letters*, Vol. 14, No. 20, 4876–4885, 2023.

[25] Leguy, A. M. A., Y. Hu, M. Campoy-Quiles, M. I. Alonso, O. J. Weber, P. Azarhoosh, M. Van Schilfgaarde, M. T. Weller, T. Bein, J. Nelson, P. Docampo, and P. R. F. Barnes, "Reversible hydration of $CH_3NH_3PbI_3$ in films, single crystals, and solar cells," *Chemistry of Materials*, Vol. 27, No. 9, 3397–3407, 2015.

[26] Song, Z., A. Abate, S. C. Watthage, G. K. Liyanage, A. B. Phillips, U. Steiner, M. Graetzel, and M. J. Heben, "Perovskite solar cell stability in humid air: Partially reversible phase transitions in the PbI_2-CH_3NH_3I-H_2O system," *Advanced Energy Materials*, Vol. 6, No. 19, 1600846, 2016.

[27] Yang, S., Y. Wang, P. Liu, Y.-B. Cheng, H. J. Zhao, and H. G. Yang, "Functionalization of perovskite thin films with moisture-tolerant molecules," *Nature Energy*, Vol. 1, No. 2, 15016, 2016.

[28] Christians, J. A., P. A. M. Herrera, and P. V. Kamat, "Transformation of the excited state and photovoltaic efficiency of $CH_3NH_3PbI_3$ perovskite upon controlled exposure to humidified air," *Journal of the American Chemical Society*, Vol. 137, No. 4, 1530–1538, 2015.

[29] Ahn, N., K. Kwak, M. S. Jang, H. Yoon, B. Y. Lee, J.-K. Lee, P. V. Pikhitsa, J. Byun, and M. Choi, "Trapped charge-driven degradation of perovskite solar cells," *Nature Communications*, Vol. 7, No. 1, 13422, 2016.

[30] Dong, X., X. Fang, M. Lv, B. Lin, S. Zhang, J. Ding, and N. Yuan, "Improvement of the humidity stability of organic-inorganic perovskite solar cells using ultrathin Al_2O_3 layers prepared by atomic layer deposition," *Journal of Materials Chemistry A*, Vol. 3, No. 10, 5360–5367, 2015.

[31] Jing, C., Z. Lin, Y. Wu, and X. Ouyang, "Air-processed perovskite solar cells: Challenges, progress, and industrial strategies," *Small*, Vol. 21, No. 35, 2504448, 2025.

[32] Liu, J., S. K. Pathak, N. Sakai, R. Sheng, S. Bai, Z. Wang, and H. J. Snaith, "Identification and mitigation of a critical interfacial instability in perovskite solar cells employing copper thiocyanate hole-transporter," *Advanced Materials Interfaces*, Vol. 3, No. 22, 1600571, 2016.

[33] Angmo, D., X. Peng, A. Seeber, C. Zuo, M. Gao, Q. Hou, J. Yuan, Q. Zhang, Y.-B. Cheng, and D. Vak, "Controlling homogenous spherulitic crystallization for high-efficiency planar perovskite solar cells fabricated under ambient high-humidity conditions," *Small*, Vol. 15, No. 49, 1904422, 2019.

[34] Yang, B., O. Dyck, J. Poplawsky, J. Keum, A. Puretzky, S. Das, I. Ivanov, C. Rouleau, G. Duscher, D. Geohegan, and K. Xiao, "Perovskite solar cells with near 100% internal quantum efficiency based on large single crystalline grains and vertical bulk heterojunctions," *Journal of the American Chemical Society*, Vol. 137, No. 29, 9210–9213, 2015.

[35] Shi, J., J. Dong, S. Lv, Y. Xu, L. Zhu, J. Xiao, X. Xu, H. Wu, D. Li, Y. Luo, and Q. Meng, "Hole-conductor-free perovskite organic lead iodide heterojunction thin-film solar cells: High efficiency and junction property," *Applied Physics Letters*, Vol. 104, No. 6, 063901, 2014.

[36] Wu, J., J.-J. Dong, S.-X. Chen, H.-Y. Hao, J. Xing, and H. Liu, "Fabrication of efficient organic-inorganic perovskite solar cells in ambient air," *Nanoscale Research Letters*, Vol. 13, No. 1, 293, 2018.

[37] Guo, S., B. Fan, S. Yao, L. Rao, S. Zhang, X. Hu, and Y. Chen, "The effect of interfacial humidity on the printing of highly reproducible perovskite solar cells in the air," *Advanced Functional Materials*, Vol. 34, No. 21, 2313715, 2024.

[38] Huang, Y., W. Zhang, Y. Xiong, Z. Yi, C. Huang, Q. Jiang, A. Basit, G. Shen, Y. Luo, X. Li, and J. Yang, "Recent advancements in ambient-air fabrication of perovskite solar cells," *Exploration*, Vol. 5, No. 3, 20240121, 2025.

[39] Tress, W., N. Marinova, T. Moehl, S. M. Zakeeruddin, M. K. Nazeeruddin, and M. Grätzela, "Understanding the rate-dependent J-V hysteresis, slow time component, and aging in $CH_3NH_3PbI_3$ perovskite solar cells: The role of a compensated electric field," *Energy & Environmental Science*, Vol. 8, No. 3, 995–1004, 2015.

[40] Eames, C., J. M. Frost, P. R. F. Barnes, B. C. O'regan, A. Walsh, and M. S. Islam, "Ionic transport in hybrid lead iodide perovskite solar cells," *Nature Communications*, Vol. 6, No. 1, 7497, 2015.

[41] Aristidou, N., C. Eames, I. Sanchez-Molina, X. Bu, J. Kosco, M. S. Islam, and S. A. Haque, "Fast oxygen diffusion and iodide defects mediate oxygen-induced degradation of perovskite solar cells," *Nature Communications*, Vol. 8, No. 1, 15218, 2017.

[42] Tsvetkov, D. S., M. O. Mazurin, V. V. Sereda, I. L. Ivanov, D. A. Malyshkin, and A. Y. Zuev, "Formation thermodynamics, stability, and decomposition pathways of $CsPbX_3$ ($X = Cl, Br, I$) photovoltaic materials," *The Journal of Physical Chemistry C*, Vol. 124, No. 7, 4252–4260, 2020.

[43] Scheidt, R. A., E. Kerns, and P. V. Kamat, "Interfacial charge transfer between excited $CsPbBr_3$ nanocrystals and TiO_2: Charge injection versus photodegradation," *The Journal of Physical Chemistry Letters*, Vol. 9, No. 20, 5962–5969, 2018.

[44] Zhang, S., S. Wu, B. H. Babu, W. Chen, R. Chen, Y. Huang, Z. Yang, H. Zhu, J. Zhou, and W. Chen, "Adverse oxidation of $CsPbI_2Br$ perovskite during the crystallization process in an N_2 glove-box," *Journal of Materials Chemistry C*, Vol. 7, No. 17, 5067–5073, 2019.

[45] Brenes, R., D. Guo, A. Osherov, N. K. Noel, C. Eames, E. M. Hutter, S. K. Pathak, F. Niroui, R. H. Friend, M. S. Islam, *et al.*, "Metal halide perovskite polycrystalline films exhibiting properties of single crystals," *Joule*, Vol. 1, No. 1, 155–167, 2017.

[46] Ren, Z., A. Ng, Q. Shen, H. C. Gokkaya, J. Wang, L. Yang, W.-K. Yiu, G. Bai, A. B. Djurišić, W. W.-F. Leung, *et al.*, "Thermal assisted oxygen annealing for high efficiency planar $CH_3NH_3PbI_3$ perovskite solar cells," *Scientific Reports*, Vol. 4, No. 1, 6752, 2014.

[47] Cheng, Y., X. Xu, Y. Xie, H.-W. Li, J. Qing, C. Ma, C.-S. Lee, F. So, and S.-W. Tsang, "18% high-efficiency air-processed perovskite solar cells made in a humid atmosphere of 70% RH," *Solar RRL*, Vol. 1, No. 9, 1700097, 2017.

[48] Chen, S., X. Xiao, H. Gu, and J. Huang, "Iodine reduction for reproducible and high-performance perovskite solar cells and modules," *Science Advances*, Vol. 7, No. 10, eabe8130, 2021.

[49] Meng, H., K. Mao, F. Cai, K. Zhang, S. Yuan, T. Li, F. Cao, Z. Su, Z. Zhu, X. Feng, *et al.*, "Inhibition of halide oxidation and deprotonation of organic cations with dimethylammonium formate for air-processed p-i-n perovskite solar cells," *Nature Energy*, Vol. 9, No. 5, 536–547, 2024.

[50] Tian, C., T. Wu, X. Zhou, Y. Zhao, B. Li, X. Han, K. Li, C. Hou, Y. Li, H. Wang, and Q. Zhang, "Air-processed efficient perovskite solar cells with full lifecycle management," *Advanced Materials*, Vol. 37, No. 1, 2411982, 2025.

[51] Yang, G., H. Gu, J. Yin, C. Fei, Z. Shi, X. Shi, X. Ying, and J. Huang, "Reductive cation for scalable wide-bandgap perovskite solar cells in ambient air," *Nature Sustainability*, 456–463, 2025.

[52] Zhang, J., J. Wu, A. Barabash, T. Du, S. Qiu, V. M. L. Corre, Y. Zhao, K. Zhang, F. Schmitt, Z. Peng, *et al.*, "Precise control of process parameters for $>$ 23% efficiency perovskite solar cells in ambient air using an automated device acceleration platform," *Energy & Environmental Science*, Vol. 17, No. 15, 5490–5499, 2024.

[53] Moazzezi, P., V. Yeddu, I. T. Cheong, M. R. Kokaba, S. Dayneko, Y. Ahmed, and M. I. Saidaminov, "Discovery of perovskite cosolvency and undoped $\mathrm{FAPbI_3}$ single-crystal solar cells fabricated in ambient air," *Journal of the American Chemical Society*, Vol. 147, No. 12, 10 203–10 211, 2025.

[54] Zhang, Y., X. Sun, Q. Wang, Y. Yue, Z. Guan, H. Liu, Z. Li, Y. Zhang, M. Qiu, D. Li, *et al.*, "Solvent environment engineering for reliable fabrication of perovskite solar cells in air with a wide humidity range," *Advanced Energy Materials*, Vol. 15, No. 27, 2500156, 2025.

[55] Ünlü, F., A. Florez, K. Dodd-Clements, L. K. Reb, M. Götte, M. Grosch, F. Yang, S. Öz, F. Mathies, S. Mathur, D. Ramírez, F. Jaramillo, and E. Unger, "Toward green processing of perovskite solar cells: Protic ionic liquids enable water- and alcohol-based $\mathrm{MAPbI_3}$ precursors inks for slot-die coating," *Advanced Energy Materials*, Vol. 15, No. 16, 2403626, 2025.

[56] Hoang, M. T., Y. Yang, N. D. Pham, and H. Wang, "Ecofriendly solution processing of perovskite solar cells using water," *The Journal of Physical Chemistry Letters*, Vol. 15, No. 26, 6880–6889, 2024.

[57] Zhai, P., L. Ren, S. Li, L. Zhang, D. Li, and S. F. Liu, "Light modulation strategy for highest-efficiency water-processed perovskite solar cells," *Matter*, Vol. 5, No. 12, 4450–4466, 2022.

[58] Lang, L., Z. Ding, Y. Du, N. Wu, P. Liu, R. Qin, S. Wang, Z. Wang, Y. Tu, X. Liu, *et al.*, "Ambient-printed methylammonium-free perovskite solar cells enabled by multiple molecular interactions," *Advanced Energy Materials*, Vol. 15, No. 21, 2405423, 2025.

[59] Zou, Y., W. Yu, H. Guo, Q. Li, X. Li, L. Li, Y. Liu, H. Wang, Z. Tang, S. Yang, *et al.*, "A crystal capping layer for formation of black-phase $\mathrm{FAPbI_3}$ perovskite in humid air," *Science*, Vol. 385, No. 6705, 161–167, 2024.

[60] Wu, G., J. Wang, X. Fang, J. Xu, X. Xia, J. Zhao, L. Zheng, M. Zhang, Z. Chen, H. Chen, L. Wang, and W. W. Yu, "Two-step inverted perovskite solar cells with $>$ 25% efficiency fabricated in ambient air," *Advanced Energy Materials*, Vol. 15, No. 27, 2500830, 2025.

[61] Liu, X., J. Zhang, H. Wang, Y. Miao, T. Guo, L. K. Ono, S. Yuan, Y. Wang, P. Ji, H. Chen, *et al.*, "$\mathrm{CsPbI_3}$ perovskite solar module with certified aperture area efficiency $>$ 18% based on ambient-moisture-assisted surface hydrolysis," *Joule*, Vol. 8, No. 10, 2851–2862, 2024.

[62] Xu, L., W. Qian, Y. Zhou, Z. Wei, H. Wang, W. Lv, J. Li, W. Huang, L. Yao, R. Chen, and W. Huang, "In situ cation exchange enables air-processed inverted perovskite solar cells with over 25% efficiency and enhanced stability," *Angewandte Chemie*, Vol. 137, No. 26, e202503702, 2025.

[63] Lu, M., J. Ding, Q. Ma, Z. Zhang, M. Li, W. Gao, W. Mo, B. Zhang, T. Pauporté, J. Zhang, *et al.*, "Dual-site passivation by heterocycle functionalized amidinium cations toward high-performance inverted perovskite solar cells and modules," *Energy & Environmental Science*, Vol. 18, 5973–5984, 2025.

[64] Chen, X., F. Yang, L. Yuan, S. Huang, H. Gu, X. Wu, Y. Shen, Y. Chen, N. Li, H.-J. Egelhaaf, *et al.*, "Perfluoroalkylsulfonyl ammonium for humidity-resistant printing high-performance phase-pure $\mathrm{FAPbI_3}$ perovskite solar cells and modules," *Joule*, Vol. 8, No. 8, 2265–2282, 2024.

[65] Song, Y., Z. Liu, X. Cai, H. Ge, X. Liu, X. Wang, A. Li, T. Miyasaka, N. Shibayama, and X.-F. Wang, "Efficient and moisture resistant wide-bandgap perovskite solar cells with phosphinate-based iodine defect passivation," *Advanced Energy Materials*, Vol. 15, No. 30, 2500650, 2025.

[66] Ning, L., Z. Yao, L. Zha, L. Song, P. Du, W.-H. Chen, and J. Xiong, "High-oriented $\mathrm{SnO_2}$ nanocrystals for air-processed flexible perovskite solar cells with an efficiency of 23.87%," *Advanced Materials*, Vol. 37, No. 27, 2418791, 2025.

[67] Zhao, Y., Y. Liu, Z. Ren, Y. Li, Y. Zhang, F.-C. Kong, T. Liu, X. Shi, Y. Dou, L. Wang, *et al.*, "Enhanced interface adhesion with a polymeric hole transporter enabling high-performance air-processed perovskite solar cells," *Energy & Environmental Science*, Vol. 18, No. 3, 1366–1374, 2025.

[68] Yang, H., Z. Xu, H. Wang, S. M. H. Qaid, O. F. Mohammed, and Z. Zang, "Iodide management and oriented crystallization modulation for high-performance all-air processed perovskite solar cells," *Advanced Materials*, Vol. 36, No. 49, 2411721, 2024.

[69] Zhu, X., D. Yu, X. Zhou, N. Wang, H. Liu, Z. Liang, C. Wu, K. Wang, D. Jin, S. Liu, and D. Yang, "Interfacial molecular anchor for ambient all-bladed perovskite solar modules," *Joule*, Vol. 9, No. 5, 101919, 2025.

[70] Han, X., X. Liu, Y. Yu, D. He, J. Feng, J. Yi, and J. Chen, "Minimizing interfacial energy losses via fluorination strategy toward high-performance air-fabricated perovskite solar cells," *Chemical Engineering Journal*, Vol. 501, 157430, 2024.

[71] Li, H., J. Duan, C. Zhang, N. Liu, L. Ma, X. Duan, J. Dou, Q. Guo, B. He, Y. Zhao, and Q. Tang, "Idealizing air-processed perovskite film competitive by surface lattice etching-reconstruction for high-efficiency solar cells," *Angewandte Chemie*, Vol. 137, No. 7, e202419061, 2025.

[72] Mali, S. S., J. V. Patil, J. A. Steele, M. K. Nazeeruddin, J. H. Kim, and C. K. Hong, "All-inorganic halide perovskites for air-processed "n-i-p" monolithic perovskite/organic hybrid tandem solar cells exceeding 23% efficiency," *Energy & Environmental Science*, Vol. 17, No. 3, 1046–1060, 2024.

[73] Hu, X., C. Zhao, Y. Liu, J.-A. Li, L. Wang, X. Tang, Y. Dou, X. Shi, T. Liu, S. Luo, and S. Chen, "Blade-coated perovskite-organic tandem solar cells in ambient conditions," *Advanced Functional Materials*, e12093, 2025.

[74] Huang, J., S. Tan, P. D. Lund, and H. Zhou, "Impact of $\mathrm{H_2O}$ on organic-inorganic hybrid perovskite solar cells," *Energy & Environmental Science*, Vol. 10, No. 11, 2284–2311, 2017.

[75] Niu, G., W. Li, F. Meng, L. Wang, H. Dong, and Y. Qiu, "Study on the stability of $\mathrm{CH_3NH_3PbI_3}$ films and the effect of post-modification by aluminum oxide in all-solid-state hybrid solar cells," *Journal of Materials Chemistry A*, Vol. 2, No. 3, 705–710, 2014.

[76] Aristidou, N., I. Sanchez-Molina, T. Chotchuangchutchaval, M. Brown, L. Martinez, T. Rath, and S. A. Haque, "The role of oxygen in the degradation of methylammonium lead trihalide perovskite photoactive layers," *Angewandte Chemie*, Vol. 127, No. 28, 8326–8330, 2015.

[77] Nazir, G., S.-Y. Lee, J.-H. Lee, A. Rehman, J.-K. Lee, S. I. Seok, and S.-J. Park, "Stabilization of perovskite solar cells: Re-

cent developments and future perspectives," *Advanced Materials*, Vol. 34, No. 50, 2204380, 2022.

[78] Said, A. A., E. Aydin, E. Ugur, Z. Xu, C. Deger, B. Vishal, A. Vlk, P. Dally, B. K. Yildirim, R. Azmi, *et al.*, "Sublimed C_{60} for efficient and repeatable perovskite-based solar cells," *Nature Communications*, Vol. 15, No. 1, 708, 2024.

[79] Li, D., Q. Lian, T. Du, R. Ma, H. Liu, Q. Liang, Y. Han, G. Mi, O. Peng, G. Zhang, *et al.*, "Co-adsorbed self-assembled monolayer enables high-performance perovskite and organic solar cells," *Nature Communications*, Vol. 15, No. 1, 7605, 2024.

[80] Asuo, I. M., D. Gedamu, N. Y. Doumon, I. Ka, A. Pignolet, S. G. Cloutier, and R. Nechache, "Ambient condition-processing strategy for improved air-stability and efficiency in mixed-cation perovskite solar cells," *Materials Advances*, Vol. 1, No. 6, 1866–1876, 2020.

[81] Lee, H. B., R. Sahani, V. Devaraj, N. Kumar, B. Tyagi, J.-W. Oh, and J.-W. Kang, "Complex additive-assisted crystal growth and phase stabilization of α-$FAPbI_3$ film for highly efficient, air-stable perovskite photovoltaics," *Advanced Materials Interfaces*, Vol. 10, No. 2, 2201658, 2023.

[82] Wang, J., G. Wang, and B. Chen, "A review of recent progress on enhancing stability of $CsPbX_3$ perovskite solar cells," *Sustainable Energy & Fuels*, Vol. 8, 4667–4686, 2024.

[83] Zheng, X., W. Kong, J. Wen, J. Hong, H. Luo, R. Xia, Z. Huang, X. Luo, Z. Liu, H. Li, *et al.*, "Solvent engineering for scalable fabrication of perovskite/silicon tandem solar cells in air," *Nature Communications*, Vol. 15, No. 1, 4907, 2024.

[84] Aihemaiti, N., Y. Jiang, Y. Zhu, and S. Peng, "Light-induced phase segregation evolution of all-inorganic mixed halide perovskites," *The Journal of Physical Chemistry Letters*, Vol. 14, No. 1, 267–272, 2023.

[85] Zhang, X., H. Huang, C. Zhao, and J. Yuan, "Surface chemistry-engineered perovskite quantum dot photovoltaics," *Chemical Society Reviews*, Vol. 54, No. 6, 3017–3060, 2025.

[86] Chen, C., J. Chen, H. Han, L. Chao, J. Hu, T. Niu, H. Dong, S. Yang, Y. Xia, Y. Chen, and W. Huang, "Perovskite solar cells based on screen-printed thin films," *Nature*, Vol. 612, No. 7939, 266–271, 2022.

[87] Bu, T., J. Li, H. Li, C. Tian, J. Su, G. Tong, L. K. Ono, C. Wang, Z. Lin, N. Chai, *et al.*, "Lead halide-templated crystallization of methylamine-free perovskite for efficient photovoltaic modules," *Science*, Vol. 372, No. 6548, 1327–1332, 2021.